Supplementary appendix: Radiomic signature accurately predicts the risk of metastatic dissemination in late-stage non-small cell lung cancer

Agata Małgorzata Wilk, Emilia Kozłowska, Damian Borys, Andrea D'Amico, Krzysztof Fujarewicz[1], Izabela Gorczewska, Iwona Dębosz-Suwińska, Rafał Suwiński, Jarosław Śmieja, Andrzej Swierniak

Supplementary Tables

Supplementary Table 1. Summary of the correlation-based feature filtering.

Feature class	All features	Features kept after correlation filtering
First order	18	6
GLCM	22	13
GLDM	14	8
GLRLM	16	10
GLSZM	16	15
NGTDM	5	4
Shape	14	9
Total	105	65

Supplementary Table 2. Potential of the data to predict EFS (clinical variables). Fisher's exact test was applied for p-value estimation.

		EFS short (N = 66)	EFS long (N = 49)	MFS short (N = 25)	MFS long (N = 49)	p-value (binary EFS)	p-value (binary MFS)
Sex	MALE	45	38	17	38	0.299	0.408
	FEMALE	21	11	8	11		
HP	SQUAMOUS	49	28	16	28	0.071	0.624
	NONSQUAMOUS	17	21	9	21		
Location	LEFT	38	27	14	27	0.850	1
	RIGHT	28	22	11	22		
T	T12	24	17	8	17	1	1
	T34	42	32	17	32		
N	N01	12	13	5	13	0.361	0.582
	N23	54	36	20	36		
Zubrod score	ZERO	17	17	6	17	0.311	0.431
	NONZERO	49	32	19	32		

Supplementary Table 3. Potential of the data to predict MFS and EFS. For binary MFS and EFS, the Mann-Whitney U test was used. For the continuous MFS log-rank test. Variables statistically significant against continuous MFS are highlighted in bold.

Feature	p-value (MFS)	p-value (EFS)	p-value (continuous MFS)
original_glcm_InverseVariance	**0.066**	**0.401**	**<0.001**
original_glszm_SizeZoneNonUniformityNormalized	**0.016**	**0.022**	**0.003**
original_glszm_SmallAreaLowGrayLevelEmphasis	**0.025**	**0.593**	**0.003**
original_glrlm_LongRunLowGrayLevelEmphasis	**0.071**	**0.555**	**0.004**
original_shape_SurfaceVolumeRatio	**0.061**	**0.115**	**0.005**
original_glszm_GrayLevelNonUniformity	**0.023**	**0.047**	**0.006**
original_glrlm_RunLengthNonUniformity	**0.011**	**0.073**	**0.007**
original_glszm_HighGrayLevelZoneEmphasis	**0.236**	**0.398**	**0.008**
original_ngtdm_Busyness	**0.020**	**0.127**	**0.009**
original_glszm_GrayLevelNonUniformityNormalized	**0.079**	**0.189**	**0.011**
original_glcm_Autocorrelation	**0.388**	**0.903**	**0.014**
original_glcm_JointAverage	**0.306**	**0.989**	**0.014**
original_glrlm_HighGrayLevelRunEmphasis	**0.357**	**0.917**	**0.014**
original_glszm_SizeZoneNonUniformity	**0.086**	**0.100**	**0.018**
original_gldm_DependenceNonUniformity	**0.037**	**0.108**	**0.019**
original_shape_MajorAxisLength	**0.087**	**0.243**	**0.022**
original_shape_LeastAxisLength	**0.135**	**0.229**	**0.023**
original_glrlm_ShortRunHighGrayLevelEmphasis	**0.495**	**0.771**	**0.024**
original_shape_Maximum2DDiameterColumn	**0.031**	**0.061**	**0.025**
original_ngtdm_Strength	**0.039**	**0.083**	**0.027**
original_shape_Maximum3DDiameter	**0.084**	**0.229**	**0.028**
original_glrlm_GrayLevelNonUniformity	**0.053**	**0.185**	**0.031**
original_glszm_LowGrayLevelZoneEmphasis	**0.056**	**0.338**	**0.031**
original_gldm_GrayLevelNonUniformity	**0.095**	**0.241**	**0.031**
original_glszm_LargeAreaLowGrayLevelEmphasis	**0.135**	**0.433**	**0.033**
original_firstorder_Range	**0.011**	**0.023**	**0.034**
original_shape_SurfaceArea	**0.067**	**0.158**	**0.037**
original_firstorder_Maximum	**0.009**	**0.026**	**0.037**
original_glszm_SmallAreaEmphasis	**0.328**	**0.953**	**0.038**
age	**0.161**	**0.255**	**0.038**
original_gldm_HighGrayLevelEmphasis	**0.369**	**0.930**	**0.039**
original_shape_Sphericity	**0.446**	**0.621**	**0.042**
original_ngtdm_Coarseness	**0.052**	**0.136**	**0.042**
original_glszm_ZoneEntropy	**0.027**	**0.019**	**0.046**
original_shape_Maximum2DDiameterSlice	0.084	0.246	0.051
original_glcm_SumEntropy	0.110	0.109	0.058
original_firstorder_MeanAbsoluteDeviation	0.006	0.015	0.063
original_firstorder_Variance	0.007	0.016	0.063
original_glcm_DifferenceVariance	0.495	0.771	0.063
original_gldm_LargeDependenceLowGrayLevelEmphasis	0.236	0.819	0.065
original_shape_MeshVolume	0.061	0.162	0.066
original_shape_VoxelVolume	0.061	0.162	0.066
original_firstorder_90Percentile	0.007	0.017	0.075

original_firstorder_InterquartileRange	0.002	0.009	0.077
original_firstorder_RobustMeanAbsoluteDeviation	0.004	0.012	0.077
original_glrlm_LongRunHighGrayLevelEmphasis	0.255	0.070	0.080
original_firstorder_RootMeanSquared	0.010	0.020	0.090
original_glcm_DifferenceEntropy	0.759	0.828	0.106
original_firstorder_Uniformity	0.154	0.047	0.118
original_firstorder_Energy	0.007	0.012	0.120
original_firstorder_TotalEnergy	0.007	0.012	0.120
original_glcm_Correlation	0.311	0.547	0.122
original_glszm_LargeAreaEmphasis	0.113	0.346	0.122
original_glszm_ZoneVariance	0.121	0.343	0.122
original_firstorder_Kurtosis	0.057	0.023	0.127
original_firstorder_Mean	0.014	0.022	0.128
original_shape_Maximum2DDiameterRow	0.140	0.335	0.132
original_glszm_LargeAreaHighGrayLevelEmphasis	0.138	0.210	0.140
original_gldm_DependenceEntropy	0.210	0.430	0.148
original_glcm_Idmn	0.785	0.953	0.189
original_shape_MinorAxisLength	0.026	0.081	0.195
original_gldm_SmallDependenceHighGrayLevelEmphasis	0.510	0.673	0.195
original_glcm_Contrast	0.716	0.881	0.213
original_glcm_MaximumProbability	0.236	0.097	0.229
original_glcm_ClusterTendency	0.171	0.481	0.256
original_glrlm_RunEntropy	0.345	0.236	0.265
original_firstorder_10Percentile	0.105	0.063	0.272
original_glcm_Imc2	0.540	0.841	0.274
original_firstorder_Entropy	0.194	0.063	0.295
original_glrlm_ShortRunLowGrayLevelEmphasis	0.295	0.682	0.301
original_glszm_ZonePercentage	0.227	0.450	0.310
original_ngtdm_Contrast	0.829	0.989	0.314
original_gldm_SmallDependenceEmphasis	0.919	0.719	0.347
original_glcm_JointEntropy	0.265	0.071	0.348
original_glrlm_RunVariance	0.179	0.355	0.348
original_glrlm_LongRunEmphasis	0.236	0.457	0.352
original_glcm_JointEnergy	0.28	0.073	0.375
original_glrlm_ShortRunEmphasis	0.642	0.890	0.382
original_glcm_DifferenceAverage	0.964	0.894	0.391
original_glrlm_LowGrayLevelRunEmphasis	0.265	0.784	0.391
original_firstorder_Median	0.021	0.021	0.400
original_glcm_ClusterShade	0.525	0.745	0.424
original_gldm_LowGrayLevelEmphasis	0.250	0.736	0.448
original_ngtdm_Complexity	0.594	0.749	0.452
original_glcm_Imc1	0.650	0.678	0.472
original_glcm_Idn	0.919	0.823	0.473
original_glrlm_GrayLevelNonUniformityNormalized	0.141	0.049	0.475
original_glrlm_RunLengthNonUniformityNormalized	0.609	0.948	0.489
original_shape_Flatness	0.751	0.819	0.494
original_gldm_SmallDependenceLowGrayLevelEmphasis	0.510	0.574	0.513
original_shape_Elongation	0.400	0.417	0.542

original_gldm_LargeDependenceHighGrayLevelEmphasis	0.642	0.379	0.549
original_glrlm_RunPercentage	0.937	0.841	0.572
original_glcm_Id	0.625	0.741	0.637
original_glszm_GrayLevelVariance	0.357	0.762	0.661
original_firstorder_Skewness	0.838	0.536	0.721
original_glcm_ClusterProminence	0.547	0.971	0.740
original_glszm_SmallAreaHighGrayLevelEmphasis	0.525	0.814	0.740
original_glcm_SumSquares	0.357	0.485	0.747
original_gldm_LargeDependenceEmphasis	1.000	0.823	0.774
original_glcm_Idm	0.777	0.784	0.795
original_firstorder_Minimum	0.407	0.452	0.858
original_gldm_DependenceNonUniformityNormalized	0.982	0.665	0.910
original_gldm_GrayLevelVariance	0.301	0.346	0.926
original_glrlm_GrayLevelVariance	0.400	0.510	0.983
original_gldm_DependenceVariance	0.601	0.780	0.983

Supplementary Table 4. Log-rank test for continuous MFS.

		N = 115	p-value (continuous MFS)
Sex	MALE	83	0.714
	FEMALE	32	
HP	SQUAMOUS	77	0.835
	NONSQUAMOUS	38	
Location	LEFT	65	0.536
	RIGHT	50	
T	T12	41	0.917
	T34	74	
N	N01	25	0.656
	N23	90	
Zubrod score	ZERO	34	0.818
	NONZERO	81	

Supplementary Figures

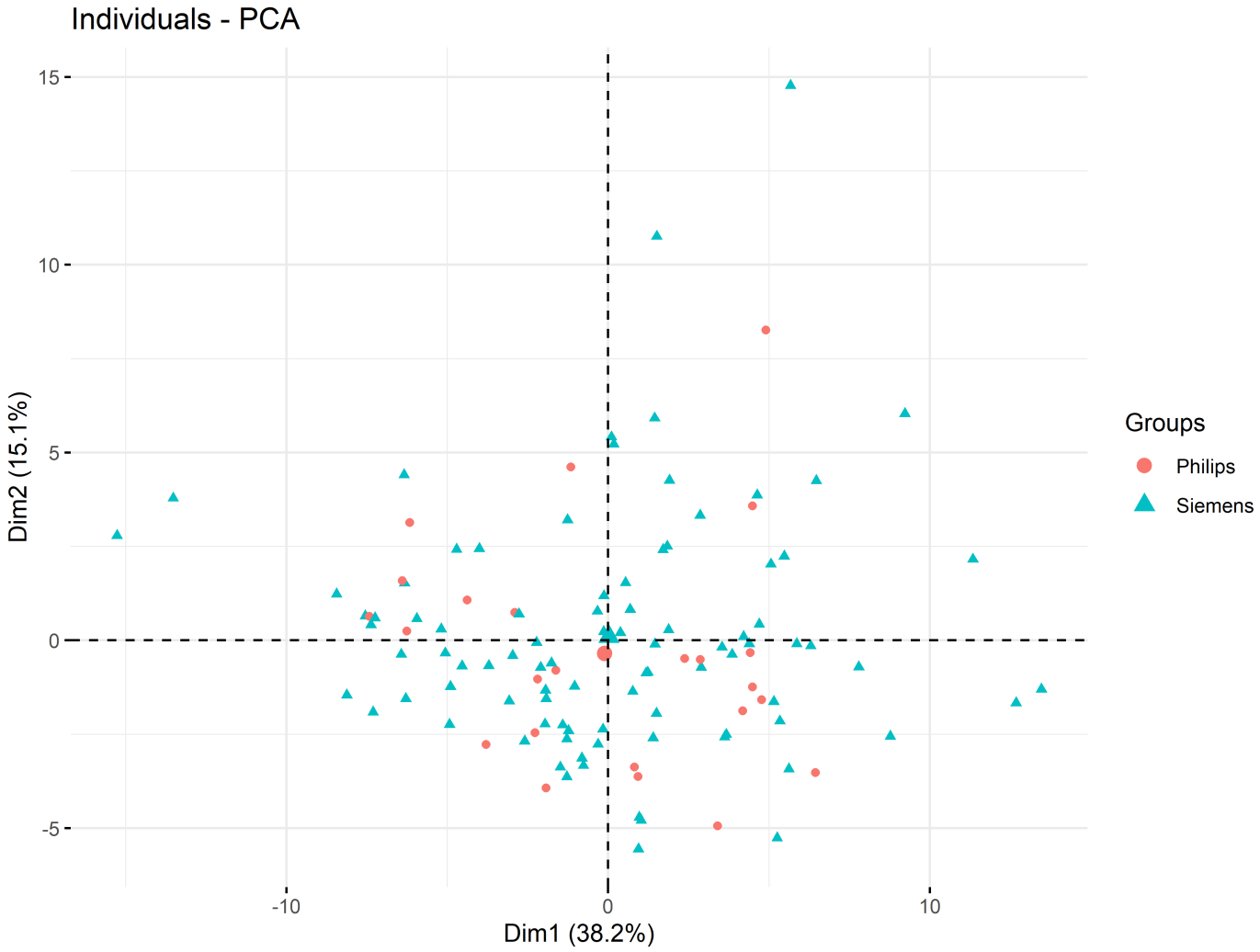

SF 1. Principal component analysis of the radiomic features (after correlation filtering). Colors correspond to the PET/CT scanner. There is no visible grouping of samples according to the scanner.

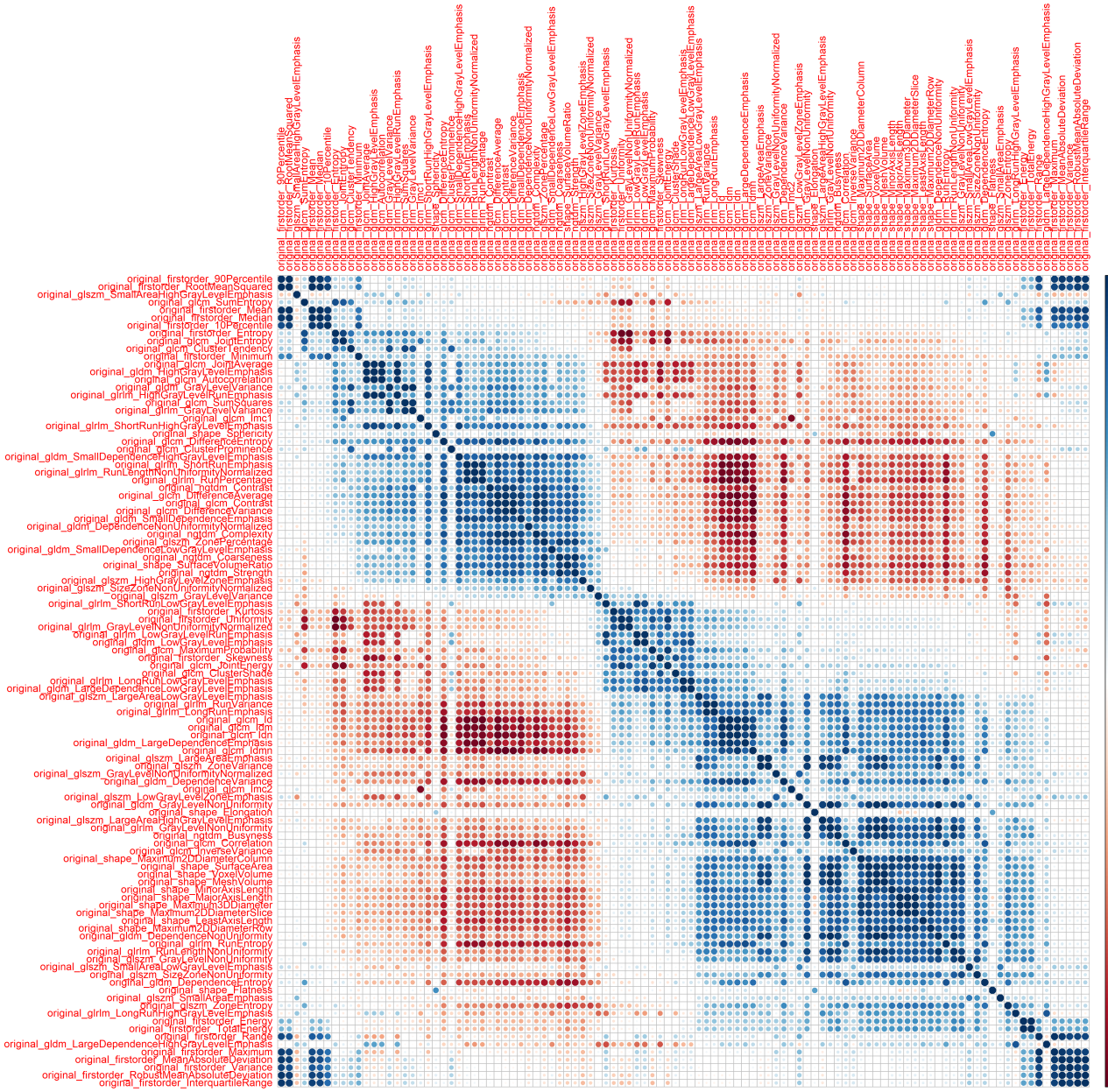

SF 2. Correlation between radiomic features.

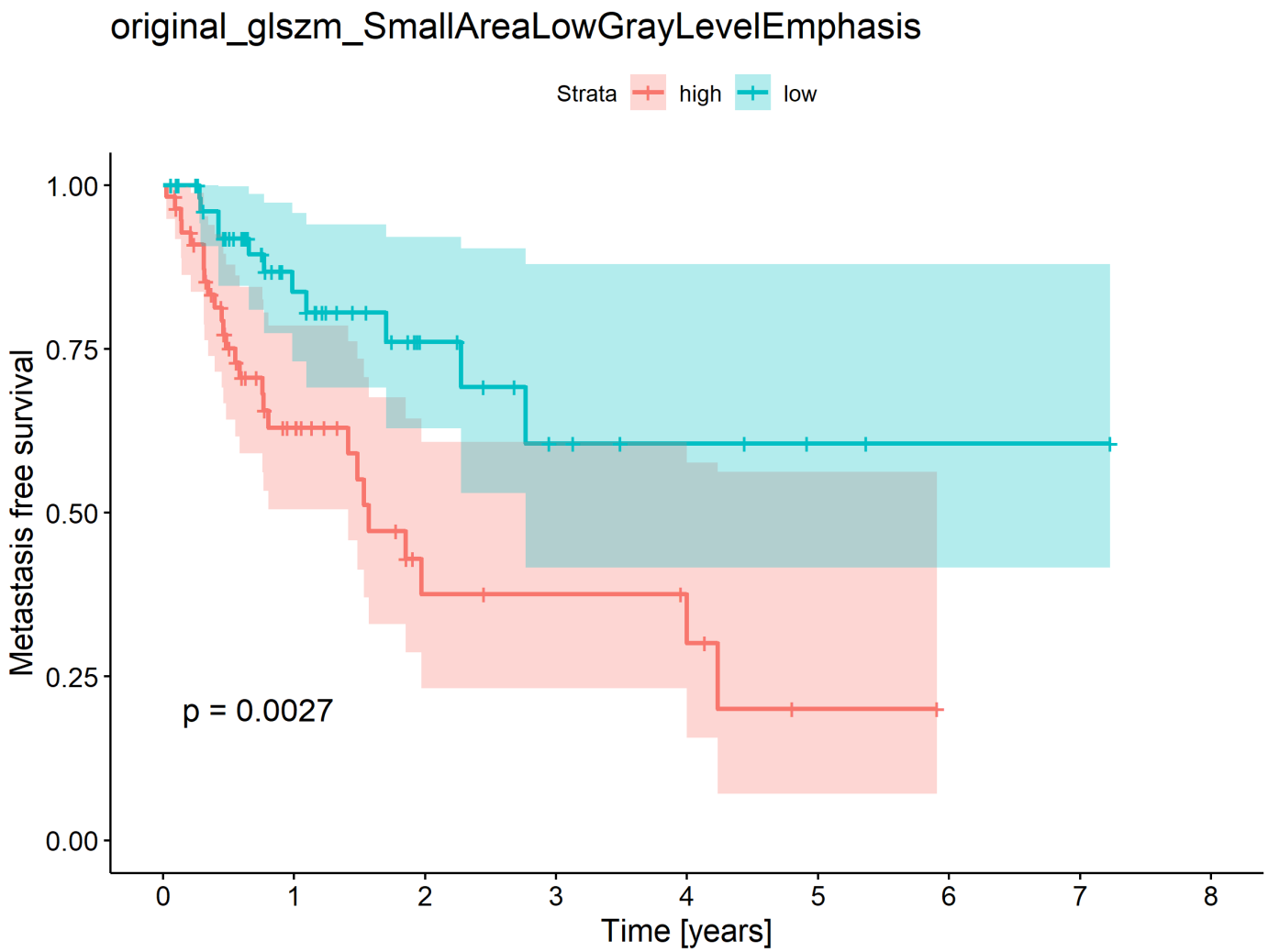

SF 3. Kaplan-Meier plot for metastatic-free survival with high/low SmallAreaLowGrayLevelEmphasis value

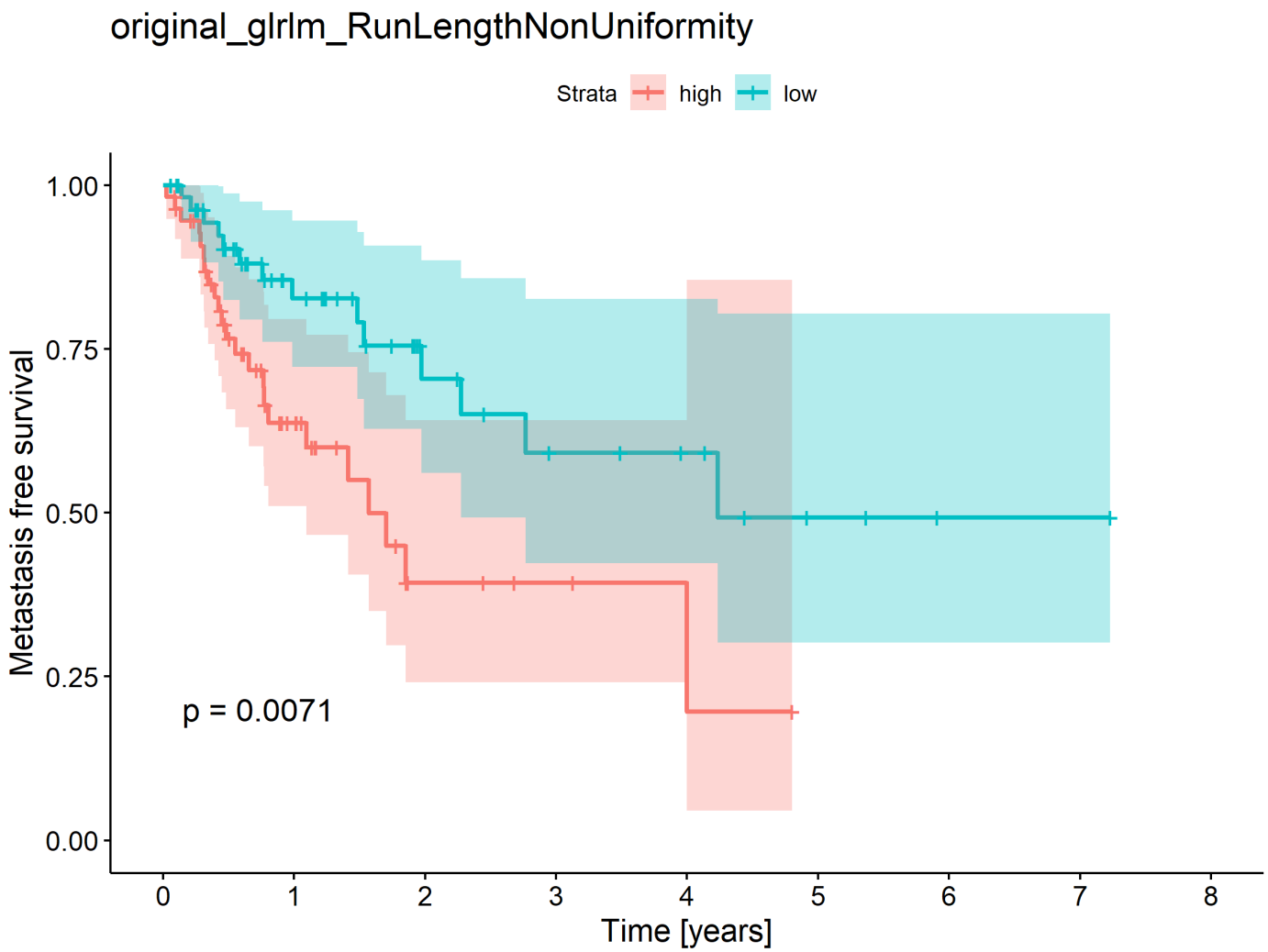

SF 4. Kaplan-Meier plot for metastatic-free survival with high/low RunLengthNonUniformity value